HHS Public Access

Author manuscript

IEEE Trans Haptics. Author manuscript; available in PMC 2019 October 01.

Published in final edited form as:

IEEE Trans Haptics. 2018 ; 11(4): 498–508. doi:10.1109/TOH.2018.2825396.

A Standard Methodology to Characterize the Intrinsic Material Properties of Compliant Test Stimuli

Gregory J. Gerling [associate professor in Systems and Information Engineering, and Biomedical Engineering],
University of Virginia, Charlottesville, VA 22904 USA (gg7h@virginia.edu).

Steven C. Hauser [graduate student in Systems Engineering],
University of Virginia, USA (sch5zc@virginia.edu).

Bryan R. Soltis [undergraduate student in Systems Engineering],
University of Virginia, USA (brs2cp@virginia.edu).

Alexis K. Bowen [graduated with her B.S. in Biomedical Engineering],
University of Virginia, USA (akb3vf@virginia.edu).

Kathryn D. Fanta [graduated with her M.E. in Systems Engineering], and
University of Virginia, USA (kdf5ph@virginia.edu).

Yuxiang Wang [graduated with his Ph.D. in Mechanical Engineering]
University of Virginia, USA (yw5aj@virginia.edu).

Abstract

Understanding how we perceive differences in material compliance, or ‘softness,’ is a central topic in the field of haptics. The intrinsic elasticity of an object is the primary factor thought to influence our perceptual estimates. Therefore, most studies test and report the elasticity of their stimuli, typically as stiffness or modulus. However, many reported estimates are of very high magnitude for silicone-elastomers, which may be due to artifacts in characterization technique. This makes it very difficult to compare the perceptual results between the studies. The work herein defines a standardized and easy-to-implement way to characterize test stimuli. The procedure involves the unconstrained, uniaxial compression of a plate into cylindrical substrates 10 mm tall by 10 mm diameter. The resultant force-displacement data are straightforwardly converted into stress-strain data, from which a modulus is readily derived. This procedure was used to re-characterize stimuli from prior studies. The revised results from the validated method herein are 200-1,100% lower than modulus values either reported and/or approximated from stiffness. This is practically significant when differences of 10-15% are perceptually discriminable. The re-characterized estimates are useful in comparing prior studies and designing new studies. Furthermore, this characterization methodology may help more readily bridge studies on perception with those designing technology.

Correspondence to: Gregory J. Gerling.

Keywords

Haptic; tactile; materials characterization; compliance; elasticity; softness

1 Introduction

TACTILE perception is studied along a number of dimensions, including compliance, amongst others such as pressure, temperature, vibration, surface roughness, texture, slipperiness, stickiness, and geometry [1]. Our ability to differentiate compliant, or 'soft,' objects is key to interacting with and manipulating naturalistic objects. When we grasp an object, our somatosensory system transforms compliance, an intrinsic material property, into percepts of 'softness' or 'hardness.' Particular relationships at the finger pad surface between force, indentation depth, and contact area are thought to encode compliance. However, investigations into the exact, underlying mechanisms remain an active research thrust, bridging neurophysiology [2], psychophysics [3], skin mechanics [4], and tactile rendering and display [5]–[8].

In such studies, the skin surface is compressed with compliant test stimuli, usually characterized via a variety of non-standard methods. The elasticity of the stimulus is thought to most prominently influence our perceptual estimates, although factors such as viscoelastic relaxation might also play a role. Therefore, a test stimulus is typically characterized by its stiffness or modulus, which are derived from force-displacement or stress-strain data, respectively. In examining the test stimuli used in prior studies, a wide range of magnitude in modulus is encountered (10 – 2,700 kPa) with upper values exceeding 2,500 kPa [2], [3], [9]–[18]. This is much stiffer than finger pad skin, which ranges from 42-130 kPa [19], [20]. Given the variety of characterization techniques and mathematical assumptions, one could question if reported compliances are accurate and/or comparable. Obtaining comparable moduli are vital in replicating a study, in particular when compliance differences of 10-15% are discriminable [17], [21].

This work develops what might become a standard methodology to characterize the compliant test stimuli employed in haptics research. The proposed methodology takes into account the range of backgrounds of its users, including non-specialists in mechanics, who might lack specialized and expensive mechanical testing equipment. It is tied as well to existing ASTM international standards. The method is described and then employed in re-characterizing test stimuli from several prior studies. In so doing, we either obtained the original stimuli or reconstructed new stimuli using similar silicone-elastomer. By describing our test stimuli in a standardized way, we can better tie together the unique studies, and ultimately our understanding of our perception of compliance.

2 Methods

This work first extracts and then summarizes the stiffness and/or modulus data from multiple prior works. In the case where only stiffness data are provided, an approximation is used to generate a modulus. Next, a compressive characterization method is introduced and demonstrated. It is demonstrated first with a small set of compliant stimuli where results are

compared against finitie element analysis and silicone-elastomers of well-reported modulus. Finally, the silicone-elastomers of the prior works are re-characterized using this technique.

2.1 Comparison of data in the literature

Several prior works have studied the perception of and/or neural responses to compliant stimuli. These studies reported stiffness and/or modulus of their test stimuli, as we summarize in Figs. 1-2. In Fig. 1, stiffness values were taken directly as reported. In contrast, modulus values were not always reported. Therefore, in Fig. 2, manuscripts which report modulus values are denoted with an asterisk.

Where not reported, we generated a modulus value by dividing the reported stiffness by the cross-sectional area of the indenter tip and multiplying it by the height of the stimulus. This is an approximation used by Bergmann Tiest, Kappers (2009) and others, as one means of extrapolating a modulus from stiffness data [17], [18]. Next, note the unique silicone-elastomer materials (Table 1) and characterization procedures (Table 2) used in prior studies. Furthermore, note that different authors report their means of mixing differently. In the case of Drewing, 2009a, the percentage values are calculated off of the total mass including diluent, rather than mass before adding diluent. Therefore, in the case of 100 grams of elastomer mixed with 50 grams of diluent one arrives at 33% diluent. Herein, those cases have been adjusted so that percentage values are based off the mass of the elastomer, so one arrives at 50% diluent.

2.2 Overview of characterization methodology

This work formulates and then demonstrates a method for characterizing elastic materials. The method involves unconstrained, uniaxial compression of a plate (24 mm dia) into cylindrical substrates (10 mm tall by 10 mm dia) and lubricated at their upper surface with mineral oil. This approach is based off of ASTM D 575-91 and ASTM D 395-17 standards, which describe test methods for rubber materials in compression [22]–[24]. Compression into the material is done at 0.5 mm/sec to a terminal force of 1 N. Resultant force-displacement data are converted to true stress-strain and then linearly fitted to generate a modulus. The method requires the simultaneous pouring of a second sample of silicone-elastomer of a precise form factor. Finite element analysis is used to verify the method's accuracy. Using this method, we re-characterize test stimuli from the prior studies noted in Methods 2.1. Furthermore, to demonstrate how particular experimental means influence modulus estimates, variations in tip diameter and substrate thickness were tested over the ranges employed in prior works.

2.3 Substrate preparation

Test stimuli of silicone-elastomer were poured into the geometry of bars (32 mm length by 107 mm width by 10 mm thick). Note that the bars' dimensions are fairly arbitrary, except for the thickness dimension of 10 mm. After seven days, two smaller, 10 mm diameter cylinders were cut from each of the bar substrates, using a biopsy punch (Robbins Instruments, RBP-100, Chatham, NJ, USA). The punch was rotated slowly by hand while being pressed gradually into the material, producing a cylindrical sample. The diameter of each sample was approximately 10 mm, although subsequent measurements at the vertical

center of the four substrates via calipers revealed slight variation, Table 3. This slight variation is due to difficulty in maintaining a consistent pressure, rotational speed, and duration in pressing the punch into the material. Prior to testing, all substrates were rinsed with a standard dish soap and cool water for 30 seconds. Then, mineral oil was dabbed onto the top of each punch. For the vast majority of cases, testing was done shortly after the punch was taken, usually within the same day.

2.4 Compressive indenter setup

To perform the uniaxial compression experiments, a Newport XPS Motion Controller (Mountain View, CA, USA) was used to control a Newport ILS-100 MVTP Linear Motion Stage. Custom software was written in Python, Version 2.7 to command displacements over an Ethernet connection. Displacement was measured by built-in functionality within the motion controller. Force was measured using a 44 N load cell (Honeywell, Model 31) that was calibrated to 0 N before each test run. Attached to the load cell were three different platen tips of diameters 2, 6 and 24 mm. The 2 and 6 mm tips were built of MACOR ceramic (Corning) filleted cylinders while the 24 mm plate was aluminum. The 24 mm platen is used for the standard characterization method, while the other two tips were used in specific, additional experiments. Upon indentation, the silicone-elastomer substrates would sit atop a 10 mm thick piece of aluminum. An example indentation of one of the substrates is shown in Fig. 3.

For each compressive indentation, the indenter was run in displacement control at a rate of 0.5 mm/sec to a terminal force of 1 N (or achieving a minimum 0.1 strain, if the substrate was stiff; typically this was no greater than 10 N). A 30 second wait time between repetitive runs allowed for consistent recovery of the materials. Note that preliminary analysis of preconditioning of the substrates showed minimal impact in successive indentations.

2.5 Data analysis and transformations

Absolute displacement of the compression platen in space (units meters) and force at the load cell (units Newtons) were sampled at a rate of 14 Hz with 27 samples per mm. These data were imported into Matlab Version 2017 (Mathworks, Natick, MA USA) for analysis. To set the point of platen to substrate contact, we used visual inspection to determine when force values consistently climbed above zero, and accordingly set displacement to zero. Data were then filtered with a 4^{th} order Butterworth filter at a cut-off frequency 1/16 of the sampling rate.

The resultant force and displacement data were converted into nominal, as well as true stress and strain data. In converting to nominal stress and strain data, the following two equations were used where σ is stress (units Pascal) and ε is strain (dimensionless quantity). Note that the original cross-sectional area (as well as length and height) of a specimen are positive in tension. However, for the case herein involving compression, they are negative.

$$\sigma_{nom} = \frac{F}{A_0} \quad (1)$$

$$\varepsilon_{nom} = \frac{l}{l_0} - 1 \quad (2)$$

In Eqns. 1-2, terms σ_{nom}, ε_{nom} stand for nominal stress and strain, F for force, A, A_0 for the original and deformed cross-sectional area, l, l_0 for the original and deformed length.

True stress and strain were formulated as follows for the cases where they are calculated, assuming perfect incompressibility and frictionless contact, Eqns. 3-4. As well, they are formulated for cases where they are directly measured via visual camera, Eqns. 5-6. Regarding the latter point, however, we note that in this work only true stress was directly measured, true strain was not. Note that all compressive stresses and strains are shown as positive for convenience of plotting.

$$\sigma_{true\_calc} = \sigma_{\text{nom}}(1 + \varepsilon_{\text{nom}}) \quad (3)$$

$$\varepsilon_{true\_calc} = \ln(1 + \varepsilon_{\text{nom}}) \quad (4)$$

$$\sigma_{true\_meas} = \frac{\text{F}}{\text{A}} \quad (5)$$

$$\varepsilon_{true\_meas} = \ln\left(\frac{l}{l_0}\right) \quad (6)$$

A linear Young's modulus (E) was fitted to each of the stress-strain curves. In particular, stress values between 0 and 0.1 strain (up to 10% deformation) were interpolated and a line was fit using least-squares regression. The slope of this line was used as the elastic modulus (units kPa).

In a redundant fashion, as a sanity check, modulus was also calculated using the material evaluation tool using ABAQUS finite element analysis software. As well, the Neo-Hookean material properties (C_{10}, D_1) were extrapolated based on the derived initial shear modulus from Young's modulus and Poisson's ratio v. Note that we used $v = 0.499$ then $4v = 5.996$ or approximately a value of 6 for the C_{10} calculation, and the D_1 value was obtained via the intermediate variable of bulk modulus K.

$$C_{10} = \frac{E}{4v} \approx \frac{E}{6} \quad (7)$$

$$D_1 = \frac{2}{K} = \frac{6(1-2v)}{E} \quad (8)$$

2.6 Experiment 1: Initial evaluation of characterization methodology

Evaluation of four silicone-elastomers.—To test the characterization methodology initially, four substrates of silicone-elastomer were examined, which had been reported previously (Gerling, 2017). They had been poured with target moduli of about 18, 22, 120 and 150 kPa. Those initial estimates had been based upon different means of characterization, using spherical indentation [25]–[28]. These values span compliances both harder and softer than fingertip skin, which range from 42-130 kPa [19], [20]. The substrates were made by use of silicone-elastomer (BJB Enterprises, TC-5005, Tustin, CA, USA) where the percentage of diluent controls their compliance, as reported in Table 1. Substrate preparation followed that of Methods 2.3.

The 24 mm diameter platen was indented into the 10 mm diameter punch substrates (4 separate target compliance pours, 2 separate punches per pour, 3 indentation replications per punch).

FEA computational validation.—We sought to verify the method's accuracy by using the measured material properties to predict the outcome of a separate indentation where a different indenter tip and substrate geometry were used. Therefore, models with two substrates and two indenter geometries were built. The first mimics the 10 mm diameter by 10 mm tall substrate and 24 mm diameter compression platen, and the second mimics a 38 mm diameter by 10 mm tall substrate and 6 mm diameter compression platen. Note that the geometry of the former follows the standard characterization methodology and the second was built to match a set of cylinders that had been used in prior study [12], [28].

The axisymmetric models and indenter tips were built in ABAQUS/CAE Version 6.14 (Dassault Systèmes, Vélizy-Villacoublay, France). For the 10 mm diameter substrate, a mesh was generated with 5,776 nodes and 5,625 elements of type CAX4RH (4-node bilinear axisymmetric quadrilateral, hybrid element, constant pressure, reduced integration, hourglass control). A penalty contact formulation was established between the platen tip and material substrate parts in the assembly to model friction. The right side of the model was unconstrained, and the centerline was constrained so that it could only move vertically upon compression. In separate simulations, the input data were derived from nominal stress-strain as well as true stress-strain. Both platen tips were modeled using analytical rigid bodies. The 24 mm diameter platen assumed a perfectly lubricated interface, while the 6 mm diameter tip assumed a frictional coefficient of 0.3 interface.

Visual tracking of cross-sectional area.—Collected over the same time course as the force-displacement data, a video (1080p HD, 30 fps) was recorded using an iPhone Model 5S (Apple, Cupertino, CA USA) to capture the change in substrate radius over the compression. Positioned in the backdrop of the visual field was a ruler with a precision of 0.2 mm. Using the video footage, the time corresponding to the greatest visual displacement was aligned with the greatest force-displacement in the data file. The time of contact between the platen and the substrate was also noted. The difference between the time of contact and greatest displacement was divided by the number of data points taken over that period. Using this value as an increment, a timeline was extrapolated between the point of contact and final reading, which was related to the change in force and displacement. Five evenly-distributed times were chosen from the timeline in the file (time of contact, final time, and three between) and found in the video. At these points in the video, the radius of the substrate was read from the ruler in the background, and placed in a column, aligning with their times. Radius values were then filled between these measurements, once again by taking the difference between two measurements and dividing by the number of points between to create an increment of change. The resultant radius values were used to calculate the changing cross-sectional area of the substrate, and in turn true measured stress. Each of the eight substrates (two punches by four compliances) was tested in this way over three replications.

2.7 Experiment 2: Evaluation of the silicone-elastomers used in prior studies

The silicone-elastomers of prior works as identified in Figs. 1 and 2 were newly poured and tested [3], [9]–[18], [29]. Each was mixed according to the diluent percentages reported in Table 1. In most cases we were able to acquire the identical brand, model, and parts of silicone-elastomer from the manufacturer as had been reported. However, in the case of LaMotte, 1995 and LaMotte, 2008, it was not possible to purchase these products [3], [16]. Therefore, different silicone-elastomer materials were formulated as substitutes, such that their stiffness matched those as they had been reported under the methods those authors employed. The newly poured and previously reported materials and their stiffness values are reported in Table A1. The original LaMotte, 2008 samples were also shipped to us for testing. In addition, Kappers, 2008 and 2009 used two different silicone-elastomers [17], [18]. Only one was able to be purchased (grey dot in Fig. 2). Several of the original samples used in those two papers were also shipped to us for testing and reported herein. These included a set representative of the full range of compliances used, with two from the 2008 paper and three from the 2009 paper. Unlike the silicone-elastomer replication we did for the LaMotte, 1995 and 2008 studies, we did not conduct a replication for those substrates of Kappers, 2008 and 2009. Basically since the 1.0 cm thick stimuli in the LaMotte papers matched the thickness of our method, it was easy to find an already poured corresponding substrate or to pour a new one. However, the substrates in the Kappers papers were much thicker, making it challenging to find a substitute. In particular, it would require trial-and-error re-pours of different silicone-elastomers at the geometry they used to back-out a similar stiffness. Another important note is that a second set of substrates were formed for re-evaluating Gerling, 2017 [12], and 2018 [29] apart from those in Figs. 1 and 2.

3 Results

3.1 Experiment 1: Initial evaluation of characterization methodology

The characterization method was evaluated first in a constrained way using four silicone-elastomer compliances, with those results validated against finite element analysis.

Evaluation of four silicone-elastomers.—Resultant force-displacement data (six indentations per each of four substrate compliances) are shown in Fig. 4. Corresponding nominal and true stress and strain are shown in Fig. 5. It is of note that the four levels of compliance in the force-displacement data are separable from each other, given multiple indentations. The modulus values derived from true stress and strain data correspond more closely with the ABAQUS fits than do the nominal stress and strain data, while not requiring any more experimental setup but just one more equation, Table 4. As well, the use of true stress and strain data yields a linear relationship over a larger range of strain. Given the two punches taken for each of four levels of compliance, we sought to estimate the between substrate consistency in modulus, Table 5.

In addition, for purposes of reference and ground truth, we measured Sylgard 184 (Dow Corning, USA) which has been measured elsewhere. We found its nominal modulus to be 1260 kPa, within the bounds of the 1320±70 kPa range published [30].

FEA computational validation.—Using ABAQUS in “nominal values” and “true values” simulations, both the nominal and true moduli derived from Fig. 5 and shown in Table 4 were separately input as material parameters into the computational model with the 24 mm diameter tip and 10 mm tall by 10 mm diameter substrate. The resultant analysis of this model and the force-displacement data it generated are compared to those as measured, Figs. 6A and B. When strains are small, the true and nominal strains are approximately equal (the nominal strain is the first order Taylor expansion of the true strain). This is to be expected since the data were derived from a substrate of similar geometry. The second procedure used the model with the 6 mm diameter tip and 10 mm tall by 38 mm diameter substrate. The results are shown in Figs. 6C and D. Likewise, the true and nominal strains were approximately equal and well approximated the case where we employed the geometry of a unique substrate and probe tip.

Visual tracking of cross-sectional area.—While true stress and strain were calculated in the above two sections, by Eqns. 3 and 4, we additionally sought to perform direct measurements of the change in cross-sectional area and the resulting impact upon stress measurements as the substrates bowed outward during compression. The visual data to capture the changes to the cross-sectional area over time were used along with Eqn. 5 to calculate true stress, as shown in Fig. 7. As is observable, accounting for the change in radius over time does linearize the data in a way similar to that achieved with the equations to attain the true stress – strain curve. Therefore, the modulus is nearly the same. That said, we did not modify nominal strain, but assumed homogeneous stress distributions.

3.2 Experiment 2: Evaluation of the silicone-elastomers used in prior studies

Figure 8 shows the measured modulus using the standard characterization method across the various stimuli recreated from the prior works noted. In comparing Fig. 8 with Fig. 2 one will note that the measured modulus values are much lower, and this is evidenced by the comparison of their values as a ratio in Fig. 9. Overall, the revised modulus values are two to eleven times lower than values either reported directly and/or approximated from stiffness.

We sought to ensure that the re-poured substrates well matched the originals, since small variance from the manufacturer or in creating the materials could lead to error. An experiment was conducted to compare a subset of stiffness values a) as reported in the original paper, b) upon our recreating of those substrates with newly poured silicone-elastomer – and tested using the procedures used by each author, and c) in characterizing some of the original stimuli now at this later point in time. This was done for the LaMotte, 1995 and 2008, Kappers, 2009, and Drewing, 2009a papers. Figure 10 gives the result of this experiment and shows that our replication of each of the stimuli closely match the original report values (compare black to grey dots). Interestingly, the data also show that those stimuli originally used in LaMotte, 2008 and Kappers, 2009 have changed over time (compare black to open circles in Fig. 10) from how they were originally reported.

3.3 Further experiments to highlight problematic techniques

Tip diameter and substrate thickness are particular experimental means that can influence material modulus, in addition to between punch and between pour variance.

Experiment on tip diameter.—Different tip sizes (0.6 cm and 2.4 cm diameter) were indented into the larger diameter substrates, 38 mm diameter by 10 mm tall to replicate others prior experiments [3], [17]. Per Figs. 11 and A1, the stress-strain curves and modulus differ significantly.

Experiment on substrate thickness.—Using a 6 mm tip and the 38 mm diameter substrates at 10 mm thick as well as 5cm thick of the same silicone material, an obvious difference is observable which impacts modulus, Fig. 12.

Comparison between-punches and between-pours.—Table 6 shows data comparing modulus values for the Gerling, 2017 and 2018 data in Exps. 1 and 2, and against the modulus previously reported using a spherical indentation procedure.

4 Discussion

A standard way of describing the test stimuli used to study compliance perception is needed to compare the results of disparate investigations. Extending upon prior ASTM standards, this work formulates and then demonstrates a methodology for characterizing the elastic compliance of silicone-elastomers. The test method was verified and validated using both physical tests and computational modeling. Then, the method was employed for test stimuli recreated from eleven prior studies. The results indicate that the revised modulus estimates are 200-1,100% lower than modulus values either reported directly and/or approximated from reported stiffness. We note that the combined errors resulting from improper

characterization techniques, or approximating modulus from stiffness, as detailed above may result in offsets of this magnitude. In addition, discrepancies of smaller magnitude can be reduced by measuring from multiple points (punches) of a sample of the same material, with multiple indentation replications per punch. By following these procedures, we find that modulus can be reliably and accurately estimated, and differentiated between test substrates that are near human perceptual discrimination thresholds.

4.1 Practical implications and materials characterization limits relative to perception

On the one hand, the prior modulus estimates in Fig. 9 are too high by about 200-1,100% when differences of 10-15% can be perceptually discriminable. This is a significant barrier to between-study comparison. On the other hand, the revised modulus estimates themselves are comparatively more similar to each other than anticipated, Fig. 8. In particular, several of the studies' compliance values are softer than that of the finger pad skin, and many compliance values are directly comparable between studies.

Moving to a finer level of analysis, very small differences in modulus can be perceptually detectable, and our method can differentiate these. For example, Gerling, 2017 showed that two sets of stimuli that differ by only 13 and 6 kPa (as noted in Table 5, "Average" comparing stimuli 1 with 2, and 3 with 4) were perceptually discriminable at a 75% threshold [12]. Given our procedure for estimating modulus, however, various sources of measurement error can exceed those differences, especially the 6 kPa difference between the two harder stimuli. Sources of measurement variance can be observed for a silicone-elastomer from mix-to-mix within a formulation, as well as from punch-to-punch within a mix, and replication-to-replication within a punch. Comparatively, for the worst case observed, mix-to-mix variance can be greater than 6 kPa where Table 6 indicates the average difference for stimulus 3 alone was 50 kPa (~30% of test substrate modulus). Likewise, replication-to-replication variance can be greater than 6 kPa where Table 5 indicates that for stimulus 4 its maximum value was 10 kPa greater than its mean (~10% of test substrate modulus). As well, the punch-to-punch variance can be greater than 6 kPa where Table 5 indicates that for stimulus 4 the difference between the averages of the two punches was 7 kPa. The stimuli used in Gerling, 2017 were found to be discriminable just above the 75% threshold, but not discriminable 100% of the time. They are, therefore, near perceptual limits. Given the exquisite sensitivity of our sense of touch it is not surprising that measurements using man-made equipment might encounter sensitivity issues before that point. That said, the defined procedure can still distinguish these two compliances, as long as the experimenter neither relies on just one punch per silicone-elastomer sample, nor a small number of replications.

Importantly, we have noted that the variance in measurement can differ between mixes of silicone-elastomer pours done at the same formulations. The origin of the observed variance, noted in particular for stimulus 3 for Gerling, 2017, was likely that the two pours were from two distinct batches of silicone-elastomers from the manufacturer, or that the mixing parts in Exp. 1 had been unused on the shelf for a period of time perhaps over 6 months or a year, or that the test stimuli in Exp. 1 were measured one year after being poured while in Exp. 2 were measured about two weeks after being poured. This highlights the need to go beyond

simply reporting mixing instructions (i.e., diluent percentages), but to report modulus. We suggest that mixing percentages might help inform an initial starting point, but that the substrate compliance cannot be reported by mixing percentages alone.

4.2 High modulus values reported previously

The majority of the 200-1,100% difference in reported-to-measured variance is tied to the use of non-standard characterization methods. In prior efforts, the compliance of the test substrates were often reported using the metric 'stiffness.' Stiffness is derived from force-displacement data and is highly dependent on diameter of the compression tip and the thickness of the substrate, as noted in Figures 11 and 12. When these are converted to modulus, significant variation in modulus is introduced because our assumptions in stress-strain calculations no longer hold. In particular, we are able to assume uniform deformation of the 10 mm dia cylindrically shaped substrate directly beneath the 24 mm dia tip. However, in the case where the compression tip is smaller in diameter than the test sample, deformation not only is observed in the substrate material directly beneath the tip, but also in the surrounding area. Such deformation is highly non-uniform. As the indenter tip diameter increases, the edge effects around the tip expand in a non-linear fashion, and dominate reaction force at the tip. Inherent material properties, modulus instead of stiffness, must be separated from an object's external form of size and shape.

That said, there are clear reasons why one might want to report stiffness. For instance, if a silicone-elastomer is already poured into a specific geometry, perhaps as part of a built device, one may not want to take a punch and destroy the device. In this case, it would be advised to pour a second sample from the same batch of silicone-elastomer at the time of pouring the irregular geometry. Outside of that possibility, one could conduct a stiffness test along the lines reported in LaMotte, 1995 and use finite element modeling of an indentation experiment with rigid indenter tips to back out the material modulus through matching force-displacement data to that observed.

4.3 True versus nominal modulus and accuracy extensions in finite element modeling

We generated moduli based upon both nominal and true stress-strain data. The two were similar, Table 4, but the true modulus was ultimately reported in Fig. 8. The rationale was that a) true modulus is based upon linear stress and strain data which makes fitting the first 0.1 deformation more straightforward, b) true stress and strain curves well fit the results of the cross-sectional imaging experiments where the area increases with greater indentation depth, c) the FEA replication study worked well with either modulus, and d) true stress and strain are more fundamental physical quantities. We often use nominal values for convenience and those work well with small deformation. In contrast, for finite (large) deformations, often the case for soft objects, the material response would always be much more accurately characterized with true stress and strain.

In this work, we employed an unconstrained compression approach. We had also considered a constrained approach, as it provides information on material compressibility, i.e., Poisson's ratio. However, we did not for two reasons. First, constrained compression is much more difficult to perform and requires a much higher precision in the fixture fabrication. For

example, the clearance between the compression plate and the fixture should be small enough to constrain the specimen, but large enough to avoid friction between the compression plate and the fixture. As a consequence, the constrained tests would be less applicable to many researchers in the field. Second, we already know that most compliant stimuli used in the past are silicone-elastomers are near incompressible and have a Poisson's ratio very close to 0.5. This assumption is accurate enough for most cases in haptics, unless the use case has confined compression and bulk modulus would need to be separately measured.

Furthermore, the characterization method presented herein works well to characterize relatively simple polymer materials such as rubbers and elastomers. Indeed as Fig. 6 indicates, at low strains, the fits to the observed data are very good, and both nominal and true derived models are about equally good predictors. However, compared to true strain, we only used a small range of data in the nominal modulus fit model, and therefore the fit at the greater levels of strain likely suffers from extrapolation error. Furthermore in Fig. 7 when the small blunt tip is used, one can see that the initial non-linear increase of force was not captured by the model. This could be due to the use of a Neo-Hookean model instead of a material model more complicated, e.g., Yeoh, Mooney-Rivlin or Ogden model. That said, by moving to more complicated material models, one increases complexity, i.e., there are more free variables to tune and justify. On the other hand, one might question why to use a Neo-Hookean instead of linear elasticity. This was done because unlike stiff objects such as steel, compliant objects usually undergo large deformations that cannot be neglected during structural analysis. For such analysis, linear material models are much less stable and will suffer from serious convergence issues during finite element analysis. By generalizing it to a hyperplastic Neo-Hookean model, we improved convergence behavior without adding new variables to introduce overfitting.

In any event, for greater accuracy for complicated nonlinear material modeling, one would have to account for the heterogeneity and anisotropy of the material, strain-dependent Poisson's ratio, viscoelasticity and plasticity, among others. Such measurements are only possible with multi-axis force measurement devices with special-purpose fixtures, non-contact extensometers, and extensive inverse FE analysis. It seems impractical for a variety of researchers in the diverse field studying compliant interactions to have access to such equipment, expertise and time resources.

4.4 Time related changes in silicone-elastomer

Finally, the silicone-elastomers appear to be changing over time. For example in Fig. 10, a set of substrates formed in about 2008 was measured in 2017 for the Kappers, 2009 data, and as well the LaMotte, 2008 data. The stiffness of those test stimuli, measured now, have changed from values reported then. The test stimuli which were initially the hardest have appeared to soften. The reasons for such change could be related to their experimental usage of being compressed into people's fingers, but may as well be going through a natural material breakdown itself. This is a point that would need to be examined longitudinally. On a shorter time scale, we have typically waited one week after pouring our samples to take

punches and test them, as we had informally noticed that this duration was required to ensure that the measurements were at a stable level.

Acknowledgments

This work was supported in part by grants from the National Institutes of Health (NINDS R01NS073119 and NINDS R01NS105241). The content is solely the responsibility of the authors and does not necessarily represent the official views of the NIH. The authors also owe a debt of gratitude to Astrid Kappers, Robert LaMotte, and Ingvars Birznieks for providing their specimens for testing, as well as to Knut Drewing and Anna Metzger for providing detailed knowledge about their procedures.

Appendix

TABLE A1

SUBSTITUTE STIMULI WERE POURED TO MATCH THOSE USED IN LAMOTTE, 1995 AND 2008

Substitute Material	Origin of Substitute Material	Stiffness LaMotte, 1995 (N/mm)	Stiffness of Substitute (N/mm)
Ecoflex 00-10	Hsiao, 2014	0.45	0.46
Alpa-sil EH VZ 11.1% Oil	Drewing, 2009a	1.75	1.72
Alpa-sil EH VZ 6.4% Oil	Drewing, 2009b	2.53	2.69

Substitute Material	Origin of Substitute Material	Stiffness LaMotte, 2008 (N/mm)	Stiffness of Substitute (N/mm)
BJB 120% Oil	n/a	0.28	0.29
BJB 100% Oil	Hauser, 2017	0.39	0.39
Elastosil M 4470 0% Oil	Kappers, 2009	2.63	2.63

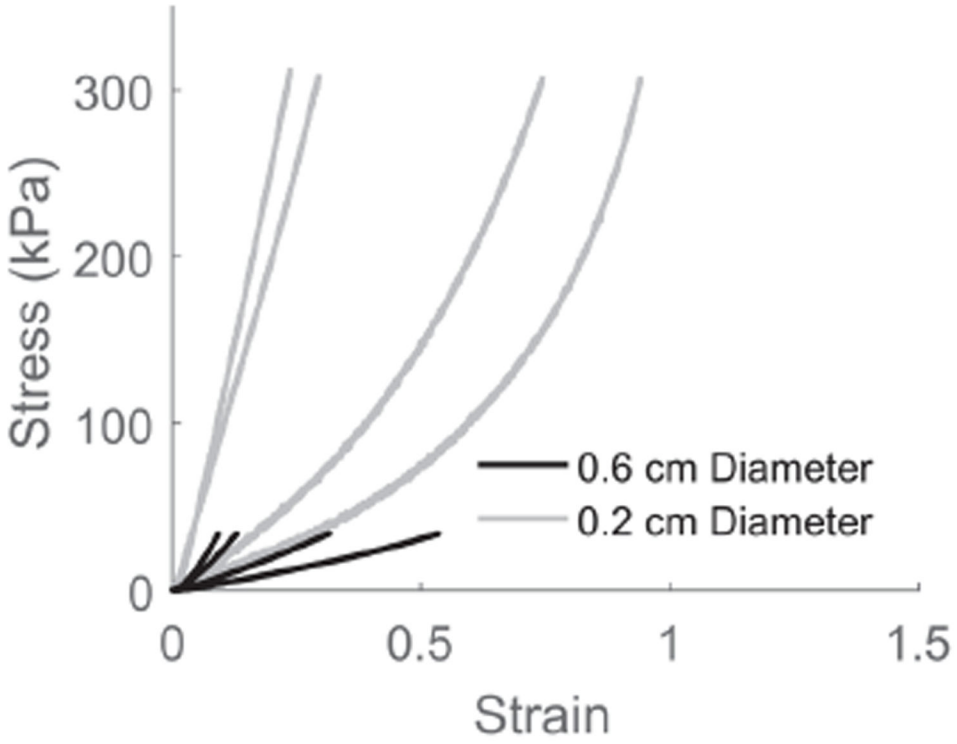

Fig. A1.

Nominal stress-strain curves compared for both 2 and 6 mm diameter tips compressed into the substrates 38 mm diameter and 10 mm tall. The nominal moduli for each line are as follows, 0.6 cm dia: 34.0, 72.0, 191.0, and 275.6 kPa; 0.2 cm dia: 100.9, 166.9, 952.5, and 984.2 kPa.

Biography

Gregory J. Gerling (S’03–M’05) received his Ph.D. degree from the Department of Mechanical and Industrial Engineering at the University of Iowa, Iowa City. He is an Associate Professor in Systems and Information Engineering, and Biomedical Engineering, at the University of Virginia. His research interests include haptics, computational neuroscience, biomechanics, and human–computer interaction.

Steven C. Hauser received the B.A. degree in Computer Science in 2014 and M.S. degree in Biomedical Engineering in 2016 from the University of Virginia. He is currently working toward his Ph.D. degree in Systems Engineering at the University of Virginia. The focus of his research is on haptics, compliance perception, and psychophysics.




Bryan R. Soltis is currently working towards his undergraduate degree in the Department of Systems and Information Engineering at the University of Virginia.




Alexis K. Bowen received the B.S. degree in Biomedical Engineering from the University of Virginia. She is currently working as a Sustaining Development Engineer in the medical device industry.

Kathryn D. Fanta received her B.S. degree in Engineering from Sweet Briar College in Amherst, Virginia and her M.E. degree in Systems Engineering from the University of Virginia.

Yuxiang Wang received his M.S. degree in Systems Engineering in 2012 and Ph.D. degree in Mechanical Engineering in 2016 from the University of Virginia. He is currently working as a Research Engineer at Align Technology. His research interests include biomechanics, medical devices, finite element analysis, and computational neuroscience.

References

[1]. Jones LA and Lederman SJ, Human hand function. Oxford University Press, 2006.

[2]. Condon M et al., “Differential sensitivity to surface compliance by tactile afferents in the human finger pad,” Journal of Neurophysiology, vol. 111, no. 6, pp. 1308–1317, 3 2014. [PubMed: 24371291]

[3]. Friedman RM, Hester KD, Green BG, and LaMotte RH, “Magnitude estimation of softness,” Experimental brain research, vol. 191, no. 2, pp. 133–142, 2008. [PubMed: 18679665]

[4]. Wang Y and Gerling GJ, “Computational Modeling Reinforces that Proprioceptive Cues May Augment Compliance Discrimination When Elasticity Is Decoupled from Radius of Curvature,” in Haptics: Neuroscience, Devices, Modeling, and Applications: 9th International Conference, EuroHaptics 2014, Versailles, France, June 24–26, 2014, Proceedings, Part II, Auvray M and Duriez C, Eds. Berlin, Heidelberg: Springer Berlin Heidelberg, 2014, pp. 360–368.

[5]. Bianchi M and Serio A, “Design and characterization of a fabric-based softness display,” Haptics, IEEE transactions on, vol. 8, no. 2, pp. 152–163, 2015.

[6]. Bicchi A, Scilingo EP, and De Rossi D, “Haptic discrimination of softness in teleoperation: the role of the contact area spread rate,” Robotics and Automation, IEEE Transactions on, vol. 16, no. 5, pp. 496–504, 2000.

[7]. Nakamura T and Yamamoto A, “Extension of an electrostatic visuo-haptic display to provide softness sensation,” in 2016 IEEE Haptics Symposium (HAPTICS), 2016, pp. 78–83.

[8]. Yazdian S, Doxon AJ, Johnson DE, Tan HZ, and Provancher WR, “Compliance display using a tilting-plate tactile feedback device,” presented at the 2014 IEEE Haptics Symposium (HAPTICS), 2014, pp. 13–18.

[9]. Cellini C, Kaim L, and Drewing K, “Visual and haptic integration in the estimation of softness of deformable objects,” Iperception, vol. 4, no. 8, pp. 516–531, Nov. 2013. [PubMed: 25165510]

[10]. Drewing K, Ramisch A, and Bayer F, “Haptic, visual and visuo-haptic softness judgments for objects with deformable surfaces,” in World Haptics 2009 - Third Joint EuroHaptics conference and Symposium on Haptic Interfaces for Virtual Environment and Teleoperator Systems, 2009, pp. 640–645.

[11]. Gwilliam JC, Yoshioka T, Okamura AM, and Hsiao SS, “Neural coding of passive lump detection in compliant artificial tissue,” Journal of Neurophysiology, vol. 112, no. 5, pp. 1131–1141, 9 2014. [PubMed: 24805077]

[12]. Hauser SC and Gerling GJ, “Force-rate Cues Reduce Object Deformation Necessary to Discriminate Compliances Harder than the Skin,” IEEE Transactions on Haptics, vol. PP, no. 99, pp. 1–1, 2017.

[13]. Kaim L and Drewing K, “Exploratory strategies in haptic softness discrimination are tuned to achieve high levels of task performance,” Haptics, IEEE Transactions on, vol. 4, no. 4, pp. 242–252, 2011.

[14]. Kaim LRand Drewing K, “Finger force of exploratory movements is adapted to the compliance of deformable objects,” in World Haptics 2009 - Third Joint EuroHaptics conference and Symposium on Haptic Interfaces for Virtual Environment and Teleoperator Systems, 2009, pp. 565–569.

[15]. Scilingo EP, Bianchi M, Grioli G, and Bicchi A, “Rendering softness: Integration of kinesthetic and cutaneous information in a haptic device,” Haptics, IEEE Transactions on, vol. 3, no. 2, pp. 109–118, 2010.

[16]. Srinivasan MA and LaMotte RH, “Tactual discrimination of softness,” Journal of Neurophysiology, vol. 73, no. 1, pp. 88–101, 1995. [PubMed: 7714593]

[17]. Tiest WMB and Kappers AM, “Cues for haptic perception of compliance,” Haptics, IEEE Transactions on, vol. 2, no. 4, pp. 189–199, 2009.

[18]. Tiest WMB and Kappers AML, “Kinaesthetic and Cutaneous Contributions to the Perception of Compressibility,” in Haptics: Perception, Devices and Scenarios, 2008, pp. 255–264.

[19]. Miguel E. Characterization of nonlinear finger pad mechanics for tactile rendering; in 2015 IEEE World Haptics Conference (WHC); 2015. 63–68.

[20]. Oprişan C, Cârlescu V, Barnea A, Prisacaru G, Olaru DN, and Plesu G, “Experimental determination of the Young’s modulus for the fingers with application in prehension systems for small cylindrical objects,” IOP Conf Ser.: Mater. Sci. Eng, vol. 147, no. 1, p. 012058, 2016.

[21]. Harper R and Stevens S, “Subjective hardness of compliant materials,’ Quarterly Journal of Experimental Psychology, vol. 16, no. 3, pp. 204–215, 1964.

[22]. “Standard Test Methods for Rubber Properties in Compression,” ASTM International, ASTM D 575–91.

[23]. “Standard Test Methods for Rubber Property—Compression Set,” ASTM International, ASTM D 395–14.

[24]. Bradley GL, Chang PC, and Mckenna GB, “Rubber modeling using uniaxial test data,” J. Appl. Polym. Sci, vol. 81, no. 4, pp. 837–848, Jul. 2001.

[25]. Carson WC, Gerling GJ, Krupski TL, Kowalik CG, Harper JC, and Moskaluk CA, “Material characterization of ex vivo prostate tissue via spherical indentation in the clinic,” Medical engineering & physics, vol. 33, no. 3, pp. 302–309, 2011. [PubMed: 21093348]

[26]. Kowalik C et al., “Construct validity in a high-fidelity prostate exam simulator,” Prostate cancer and prostatic diseases, vol. 15, no. 1, pp. 63–69, 2012. [PubMed: 21860409]

[27]. Baumgart LA, Gerling GJ, and Bass EJ, “Characterizing the range of simulated prostate abnormalities palpable by digital rectal examination,” Cancer epidemiology, vol. 34, no. 1, pp. 79–84, 2010. [PubMed: 20061202]

[28]. Hauser SC and Gerling GJ, “Measuring tactile cues at the fingerpad for object compliances harder and softer than the skin,” presented at the 2016 IEEE Haptics Symposium (HAPTICS), 2016, pp. 247–252. [PubMed: 27331072]

[29]. Hauser SC and Gerling GJ, “Imaging the 3-D defor-mation of the finger pad when interacting with compliant materials,” presented at the 2018 IEEE Haptics Symposi-um (HAPTICS), 2018, pp. 7–13.

[30]. Johnston ID, McCluskey DK, Tan CKL, and Tracey MC, “Mechanical characterization of bulk Sylgard 184 for microfluidics and microengineering,” J. Micromech. Microeng, vol. 24, no. 3, p. 035017, 2014.

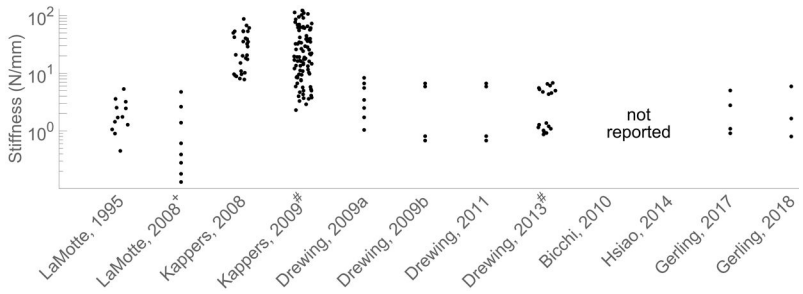

Fig. 1.

Stiffness values reported in several prior works. A plus '+' sign indicates that the same stimuli were used as reported in Birznieks, 2014. A pound '#' sign indicates that the authors used two different methods to measure their stimuli stiffness, from which the modulus values were derived. Note that Drewing, 2009a refers to "Haptic, visual and visuo-haptic softness judgments for objects with deformable surfaces."

Note that authors' last names represent the most senior leader of a given lab.

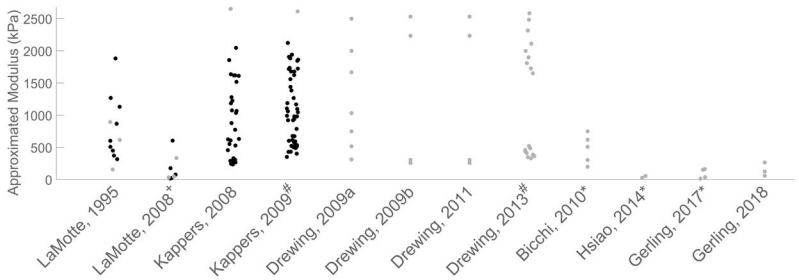

Fig. 2.

Modulus either directly reported in, or approximated/extrapolated from the stiffness reported in, each respective paper according to the procedure in Methods 2.1. A plus '+' sign indicates the same stimuli were used as reported in Birznieks, 2014. A pound '#' sign indicates that the authors used two different methods to measure their stimuli stiffness, from which the modulus values were derived. An asterisk '*' denotes that modulus values were explicitly stated within the paper, while the moduli values for the other papers were approximated/extrapolated from stiffness measurements. Dot color is used for comparison to Figure 8. Gray dots indicate a stimulus of comparison to Figure 8, black indicates a stimulus that the authors reported but for which we did not generate a revised modulus.

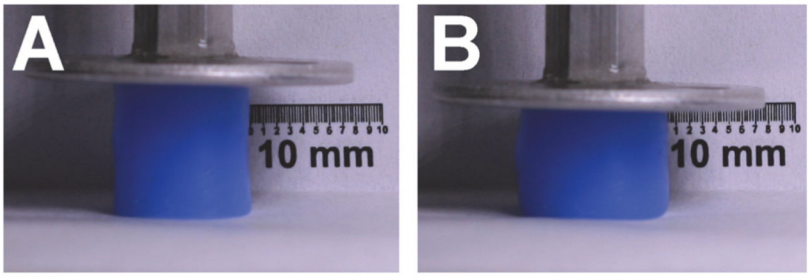

Fig. 3.

Indentation of a single punch substrate, at A) initial contact and B) partial deformation. The ruler in the background shows units of 0.2 mm.

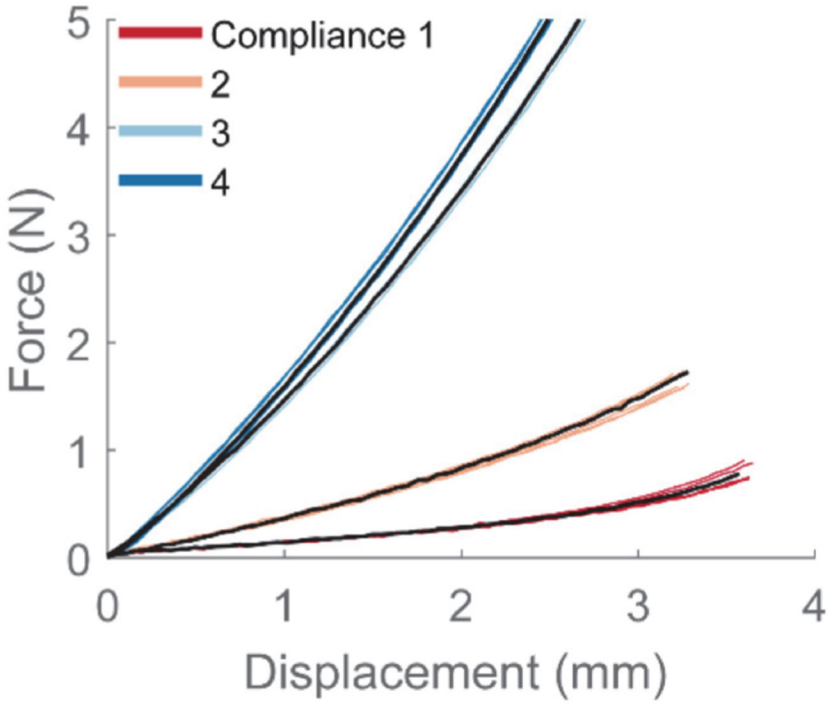

Fig. 4.

Force-displacement data from multiple replications with each of the four compliances of Exp. 1. The 24 mm diameter plate was compressed into the 10 mm tall by 10 diameter punch substrates. Trials near the mean are shown in black and referred to in the subsequent figures.

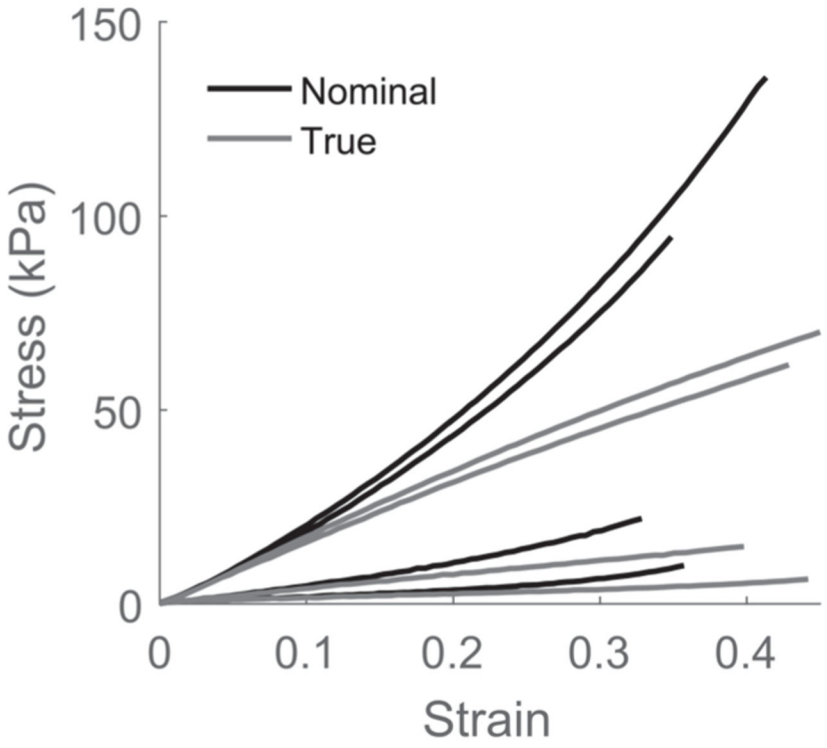

Fig. 5.

Stress-strain curves, both nominal and true calculated, for all four compliances. The 24 mm diameter flat plate was compressed into the 10 mm tall by 10 mm diameter punch substrates. The moduli for each line are as follows, nominal: 16.5, 41.0, 164.8, and 176.0 kPa; true: 15.2, 38.0, 153.2, and 163.4 kPa.

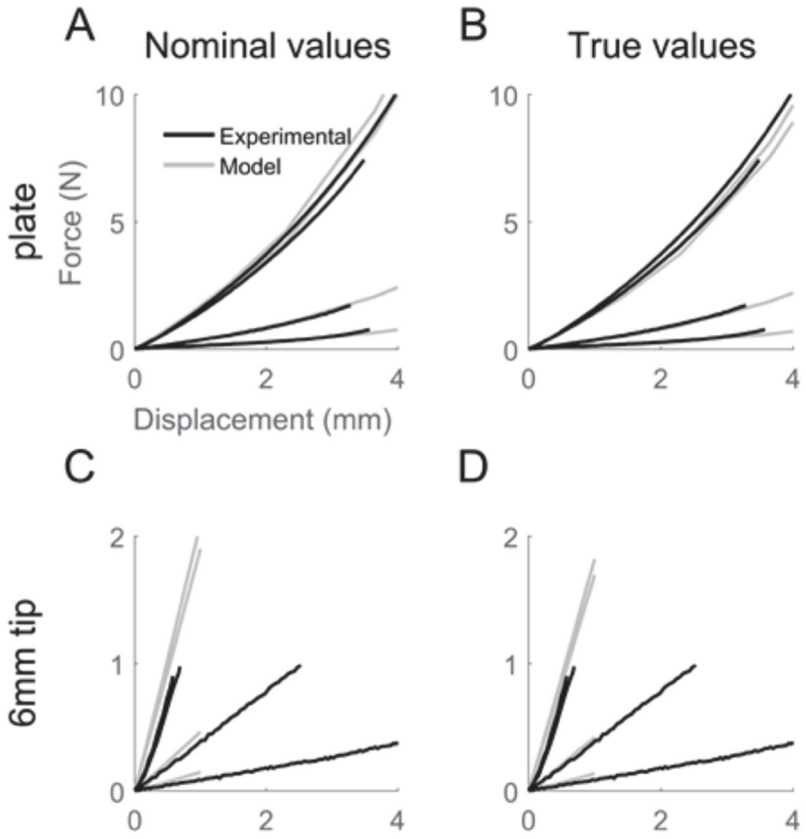

Fig. 6.

Measured force-displacement relationship compared to finite element model predictions. Panels A and B are for the 24 mm diameter flat plate with the 10 mm tall by 10 diameter punch substrates, while Panels C and D are for the 6 mm diameter tip with the 10 mm tall by 38 diameter substrates. Predictions based upon FE material models build from both nominal and true calculated stress-strain values are shown to be nearly the same.

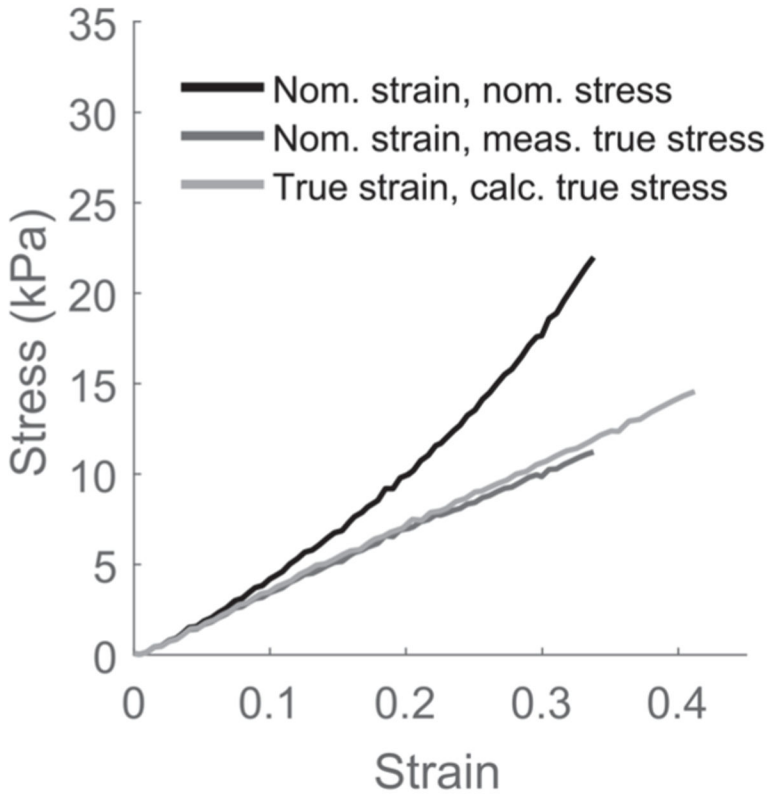

Fig. 7.

Stress-strain curves comparing the nominal stress-strain data with true stress-strain data as well as nominal strain, true stress data measured from visual inspection of the cross-sectional area. The moduli for each line are as follows, nominal strain with nominal stress: 33.3 kPa, nominal strain with measured true stress: 30.1 kPa, true strain with calculated true stress: 30.7 kPa.

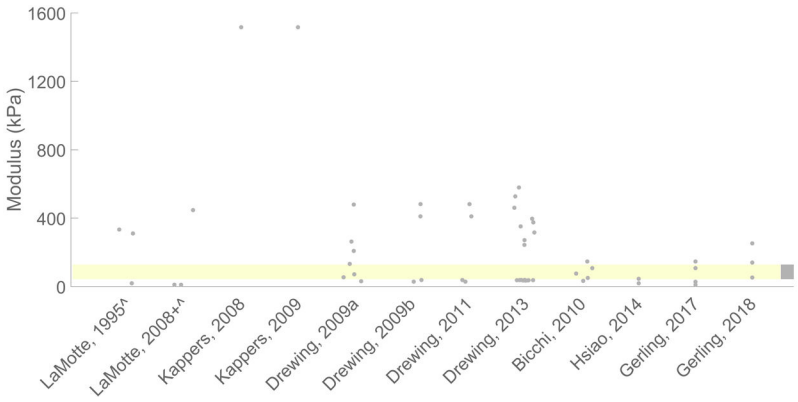

Fig. 8.

True modulus values measured via the standard characterization method of various stimuli recreated from prior works. The yellow highlighted area (marked redundantly with a gray line at the rightmost of the figure) indicates a range of 42-130 kPa, approximating human finger pad skin (reference). A plus '+' sign indicates that the same stimuli were used as reported in Birznieks, 2014. A caret '^' sign indicates that a stimuli of a different silicone-elastomer composition was used as a substitute for one that could not be acquired or is no longer produced. Note its validation was done in Fig. 10.

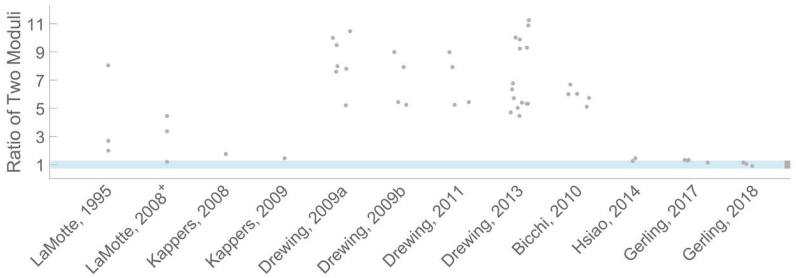

Fig. 9.

Ratio of reported modulus from Fig. 2 to measured modulus from Fig. 8. For example, a ratio of 2 indicates the paper's modulus was twice our measured value. The blue highlighted area (marked redundantly with a gray line at the rightmost of the figure) indicates a ratio of one, plus and minus 10%. A plus '+' sign indicates that the same stimuli were used as reported in Birznieks, 2014. Note that Kappers 2008 and 2009 involve the same stimuli but use different characterization methods.

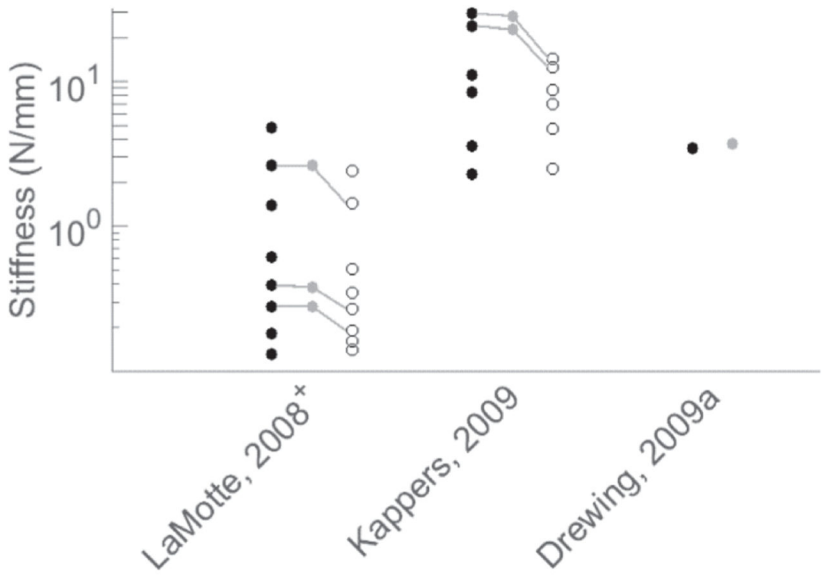

Fig. 10.

Stiffness values comparing (black closed circles) originally reported stiffness, (grey circles) stiffness of our recreated substrate, and (open circles) retest of the original stimulus at this later point of time. Note that there are six data points for the Kappers, 2009 substrates because the authors of that paper made estimates using two different characterization methods, and we followed similarly. Where applicable, grey lines connect the same stimuli.

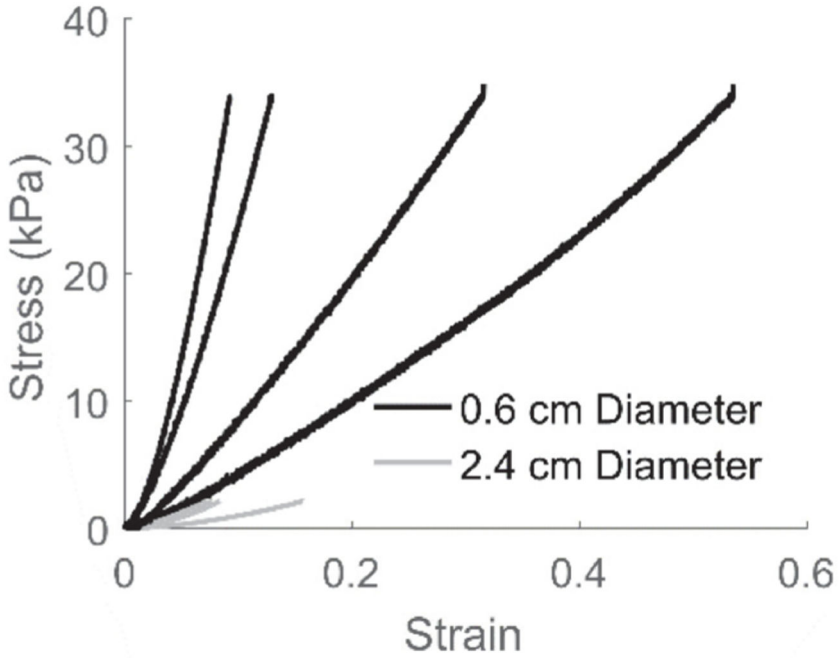

Fig. 11.

Nominal stress-strain curves compared for both 6 and 24 mm diameter tips compressed into the substrates 38 mm diameter and 10 mm tall. The nominal moduli for each line are as follows, 0.6 cm dia: 34.0, 72.0, 191.0, and 275.6 kPa; 2.4 cm dia: 6.6, 17.8, 21.8, and 27.2 kPa.

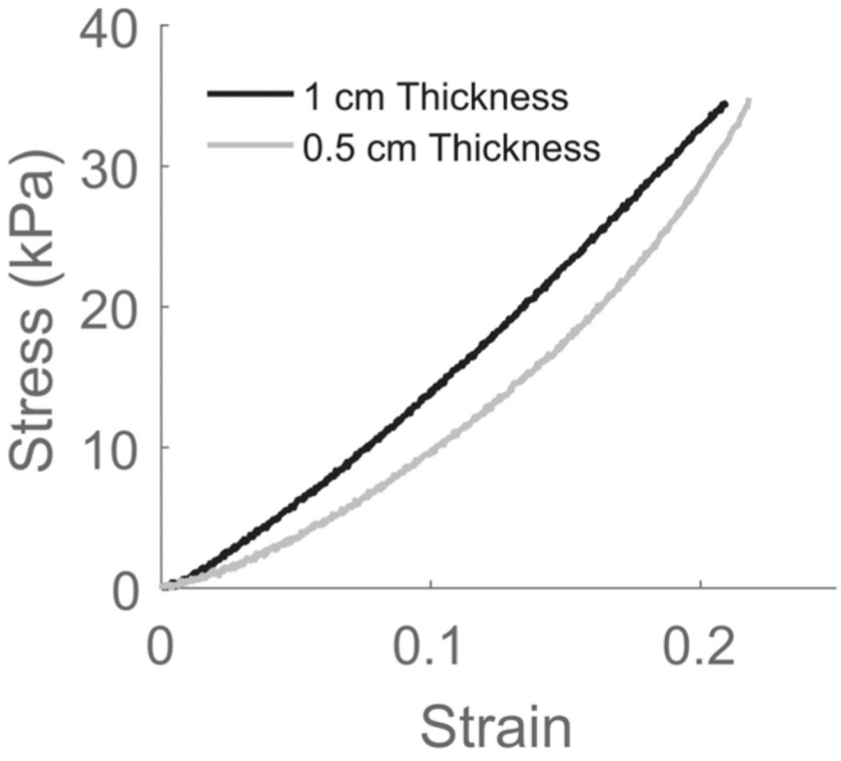

Fig. 12.

Nominal stress-strain curves comparing the effects of changing substrate thickness for one compliance (#3 from Exp.1)given a small tip indenter into a larger substrate. The 6 mm diameter tip was compressed into the 38 mm diameter by 10 mm tall substrates. The moduli for each line are as follows, 1 cm thick substrate: 126.1 kPa, 0.5 cm thick: 72.7 kPa.

TABLE 1

REFERENCED PAPERS AND THEIR ELASTOMER AND DILUENT PROPERTIES. PERCENT DILUENT IS GIVEN AS PERCENT DILUENT OF ELASTOMER (I.E., 100 G OF ELASTOMER MIXED WITH 50 G OF DILUENT IS 50% DILUENT).

Author, Year	Silicone-Elastomer	Diluent	Percent Diluent	Manufacturer	Location
LaMotte, 1995	GE RTV 615	RTV 910	n/a	General Electric (RTVs)	Boston, MA, USA
LaMotte, 2008	GE RTV 615, 6126 6136, 6156	47 V Silicone Fluid (615 only)	n/a	General Electric (RTVs) The Smith Group, Inc. (47 V)	Boston, MA, USA Warminister, PA, USA
Kappers, 2008	Elastosil M 4470	n/a	n/a	Wacker	Munich, Germany
Kappers, 2009	Elastosil M 4470	n/a	n/a	Wacker	Munich, Germany
Drewing, 2009a	Alpa-sil EH VZ (Modasil Extra)	ALPA-OIL-50 (Silicone oil V50)	0 ǀ 11.1 ǀ 25 ǀ 42.9 ǀ 66.7 ǀ 100 ǀ 150	Modulor	Montlingen, CH (Berlin, Germany)
Drewing, 2009b	Alpa-sil EH VZ	ALPA-OIL-50	6.4 ǀ 11.1 ǀ 135.6 ǀ 150	Modulor	Montlingen, CH
Drewing, 2011	Alpa-sil EH VZ	ALPA-OIL-50	6.4 ǀ 11.1 ǀ 135.6 ǀ 153.2 5.8 ǀ 7.2 ǀ 9.6 ǀ 13.6 ǀ 16.3 ǀ 19 ǀ 22 ǀ	Modulor	Montlingen, CH
Drewing, 2013	Alpa-sil EH VZ	ALPA-OIL-50	25 ǀ 28.2 ǀ 117.4 119.8 ǀ 123.5 ǀ 124.7 ǀ 128.6 ǀ 131.2 ǀ 133.9 ǀ 136.7 ǀ 140.4	Modulor	Montlingen, CH
Bicchi, 2010	BJB TC-5005 A/B mix	BJB TC-5005 C	0 ǀ 10 ǀ 20 ǀ 35 ǀ 45 ǀ 50	BJB Enterprises	Tustin, CA, USA
Hsiao, 2014	Ecoflex 00-10 Ecoflex 00-30	n/a	n/a	Smooth-On	Macungie, PA, USA
Gerling, 2017	BJB TC-5005 A/B mix	BJB TC-5005 C	0 ǀ 10 ǀ 80 ǀ 100	BJB Enterprises	Tustin, CA, USA
Gerling, 2018	Cell Guard A/B mix	Silicone oil V50	0 ǀ 75 ǀ 125	ML Solar, LLC Modulor	Campbell, CA, USA Berlin, Germany

TABLE 2

REFERENCED PAPERS AND THEIR METHODS FOR INDENTING AND MEASURING STIMULI VALUES, AS WELL AS THE PHYSICAL DIMENSIONS OF THE STIMULI THEMSELVES. THE ASTERISKS '*' INDICATES WHICHEVER WAS REACHED FIRST.

Paper			Probe			Stimuli	
Author, Year	**Area (mm^2)**	**Geometry**	**Indention Rate**	**Terminal Force (N)**	**Terminal Depth**	**Height (mm)**	**Area (mm^2)**
LaMotte, 1995	28.3	circular	0.5 mm/s	0.981	n/a	10	962
LaMotte, 2008	78.5	circular	0.5 mm/s	1.25*	7 mm*	10	962
Kappers, 2008	100	circular	manually controlled	not given	not given	40	1320
Kappers, 2009	100 1320	circular	1.0 N/s	20 50	n/a	20 40	1320
Drewing, 2009a	100	circular	not given	13	n/a	<30	1590
Drewing, 2009b	100	circular	manually controlled	9	n/a	38	4418
Drewing, 2011	100	circular	manually controlled	9	n/a	38	4418
Drewing, 2013	100	circular	manually controlled	9 (soft stimuli) 29 (hard stimuli)	n/a	38	4418
Bicchi, 2010	177	circular	manually controlled	not given	not given	7	1075
Hsiao, 2014	not given	not given	20-80 mm/s	n/a	varied	35	1225
Gerling, 2017	452	circular	0.5 mm/s	1	n/a	10	78.5
Gerling, 2018	452	circular	0.5 mm/s	1	n/a	10	78.5

TABLE 3

DIAMETER (MM) OF THE PUNCHED SUBSTRATES IN EXP. 1

Compliance	1	2	3	4
Punch 1	10.18	9.92	10.10	9.91
Punch 2	10.16	9.98	9.95	10.01

TABLE 4

MODULI (KPA) AS OBTAINED USING NOMINAL, TRUE CALCULATED AND ABAQUS FITTED STRESS AND STRAIN DATA.

Compliance	1	2	3	4
Nominal	14.8	39.7	159.9	176.7
True	13.4	36.4	157.6	163.1
ABAQUS	12.4	38.9	156.7	168.3

TABLE 5

AVERAGE TRUE MODULI (KPA) DERIVED FROM TRUE STRESS-STRAIN WITH STANDARD DEVIATION, SHOWING THE LEVEL OF VARIABILITY BETWEEN THE TWO PUNCHES AND THREE INDENTATION REPLICATIONS PER PUNCH.

Compliance	1	2	3	4
Punch 1	14.3±0.9	37.8±2.6	153.6±12.0	159.6±3.4
Punch 2	12.5±0.3	35.1±2.3	159.9±0.0	166.5±13.7
Average	13.4±1.1	36.4±2.7	157.6±12.8	163.1±9.7
Max	15.1	40.3	166.1	176.3

TABLE 6

Impact of Mix-To-Mix Differences on True Modulus (kPa, with standard deviation) For Same Formulations between Exps. 1 and 2. Shown also is Prior Spherical Indentation Data, From Gerling, 2017

Compliance	1	2	3	4
Exp. 1	13.4±1.1	36.4±2.7	157.6±12.8	163.1±9.7
Exp. 2	11.0±1.6	28.1±1.2	108.1±4.8	146.8±5.5
Spherical indentation	18.0	22.0	120.0	150.0